Reaction of Aromatic *N*-Oxides with Dipolarophiles. XV. Formation of the 1,5-Sigmatropy Products and Their Double Ene Reaction Products

Toshikazu MATSUOKA, Kikuma ONO, Kazunobu HARANO and Takuzo HISANO*

Faculty of Pharmaceutical Sciences, Kumamoto University, 5–1 Oe-honmachi, Kumamoto 862, Japan. *Received May 14, 1990*

In connection with the pericyclic reaction of 3,5-dimethylpyridine *N*-oxide with *N*-substituted maleimides, the structure of a 1,5-sigmatropy product was determined by the X-ray crystallographic method. In the reaction of 2-alkylpyridine *N*-oxides with *N*-substituted maleimides, we have isolated a series of 1:3 ene reaction products of a new type.

The primary *exo* cycloadducts readily transform into the *endo* 1,5-sigmatropic rearrangement products, which again react with two molecules of *N*-substituted maleimide to give the 1:3 ene reaction products. The observed reaction behavior and plausible reaction pathways are discussed in terms of frontier molecular orbital considerations.

Keywords pericyclic reaction; MNDO frontier molecular orbital; charge transfer complex; X-ray analysis; pyridine *N*-oxide; *N*-phenylmaleimide; 1:3 ene reaction product; ene reaction

Cycloaddition reactions have figured prominently in both synthetic and mechanistic chemistry. In the past decade, we have examined the 1,3-dipolar cycloadditions of aromatic *N*-oxides (I) with aryl isocyanates and clarified several controlling factors in the 1,3-dipolar reaction based on kinetic data and molecular orbital calculation.[1] In the reaction, the stereochemistry of the cycloaddition could not be established, because the isocyanates have a linear structure and both *exo* and *endo* addition give the same product.

Recently, we reported the 1,3-dipolar cycloaddition of 3,5-dimethylpyridine *N*-oxide (Ia) with *N*-substituted maleimides (II), and discussed the stereochemistry of the transition state. The cycloaddition afforded the *endo* 2,3-dihydrofuro[3,2-*b*]pyridine-type cycloadducts (III) arising from 1,5-sigmatropic rearrangement of primary *exo* cycloadducts.[2] This makes a striking contrast to the results obtained in the cycloadditions of some nitrones such as *N*,α-diphenylnitrone with II, wherein the *endo* cycloadditions were mainly observed.[3a]

In this connection, we have reported an X-ray analysis[4] of the 1,5-sigmatropic rearrangement product derived from the cycloadduct of 3,5-dimethylpyridine *N*-oxide and *N*-butylmaleimide. In this paper, we describe the 1,3-dipolar cycloaddition of various alkylpyridine *N*-oxides (Ia—h) with *N*-substituted maleimides (IIa—i). The results are discussed here in detail in comparison with the previous work and additional data that we have obtained.

Results

Cycloaddition of 3,5-Dimethylpyridine *N*-Oxide (Ia) with *N*-Substituted Maleimides (II) To Examine the generality of the *exo* cycloaddition, the 1,3-dipolar cycloadditions of Ia with II were performed. The yields and spectral data for the products are summarized in Tables I and II.

As can be seen in Table I, the mass spectra (MS) of the products (III) showed molecular peaks corresponding to the 1:1 adducts. The infrared (IR) spectra of III exhibited characteristic absorptions of a cyclic imido carbonyl group in the vicinity of 1715 cm^{-1}. The proton nuclear magnetic resonance (^{1}H-NMR) spectra showed two methyl signals as a singlet and a weakly split singlet due to allylic coupling. Three angular methine protons appeared as an ABX pattern. Inspection of the coupling constants indicates that the three protons are oriented in *cis* disposition. This suggests that the primary cycloadditions proceed *via exo* transition states (see Chart 1).

X-Ray Analysis of the 1,5-Sigmatropic Rearrangement Product In general, 1,3-dipolar cycloadditions of nitrones and azomethine imines involving the phenanthridine skeleton give mainly *endo* primary cycloadducts.[3a,b] Stereoselective *exo*-cycloaddition has scarcely been observed in the field of cycloaddition. So far as we know, there are only a few examples of the *exo*-cycloaddition of pyridine *N*-oxides.

Therefore, we performed a single crystal X-ray analysis. Suitable single crystals could be obtained only in the case

TABLE I. Cycloadducts (IIIa—k) from the 1,3-Dipolar Reaction of 3,5-Dimethylpyridine *N*-Oxide (Ia) with *N*-Substituted Maleimides (IIa—k)[a]

Adduct[b]	R	Yield (%)	mp (°C)	Formula	High-resolution MS Calcd (Found)	IR (cm^{-1}) C=O
IIIaa	Ph	40.2	172.5—173.5	$C_{17}H_{16}N_2O_3$[c]		1715
IIIab	*p*-ClC_6H_4	25.2	209	$C_{17}H_{15}ClN_2O_3$[c]		1710
IIIac	*p*-MeC_6H_4	40.2	187—188	$C_{18}H_{18}N_2O_3$[c]		1715
IIIad	*p*-FC_6H_4	42.5	187—188	$C_{17}H_{15}FN_2O_3$	314.1067 (314.1096)	1716
IIIae	*m*-FC_6H_4	41.8	135—137	$C_{17}H_{15}FN_2O_3$	314.1067 (314.1113)	1714
IIIaf	*o*-FC_6H_4	43.1	152—153	$C_{17}H_{15}FN_2O_3$	314.1067 (314.1096)	1724
IIIag	*p*-Cl, *o*-FC_6H_3	26.7	187—188	$C_{17}H_{14}ClFN_2O_3$	348.0667 (348.0656)	1724
IIIah	*m*-Cl, *p*-FC_6H_3	10.3	153—154	$C_{17}H_{14}ClFN_2O_3$	348.0667 (348.0666)	1722
IIIai	*o*-Cl, *p*-FC_6H_3	25.3	187—190	$C_{17}H_{14}ClFN_2O_3$	348.0667 (348.0661)	1724

a) Refluxed for 10 h in toluene. IIIaa, IIIab and IIIac: see ref. 2*b*. *b*) Colorless needles, recrystallized from C_6H_6. *c*) Analyzed for C, H and N; the results were within ±0.3% of theoretical values.

TABLE II. ^{1}H-NMR Spectral Data for the Cycloadducts (III)

Comp. No.	^{1}H-NMR δ (400 MHz, in $CDCl_3$)
IIIad	1.35 (3H, s, C_{8a}-Me), 1.87 (3H, d, J=1.8 Hz, C_7-Me), 4.10 (1H, dd, J=9.3, 8.0 Hz, C_{4a}-H), 4.35 (1H, dd, J=9.3, 2.2 Hz, C_{4b}-H), 4.93 (1H, d, J=8.0 Hz, C_{1a}-H), 5.93 (1H, dd, J=2.2, 2.2 Hz, C_8-H), 7.10—7.42 (4H, m, aromatic CH), 7.82 (1H, dd, J=2.2, 2.2 Hz, C_6-H)
IIIae	1.34 (3H, s, C_{8a}-Me), 1.87 (3H, d, J=2.2 Hz, C_7-Me), 4.11 (1H, dd, J=9.5, 8.0 Hz, C_{4a}-H), 4.35 (1H, dd, J=9.5, 2.2 Hz, C_{4b}-H), 4.93 (1H, d, J=8.0 Hz, C_{1a}-H), 5.93 (1H, dd, J=2.2, 2.2 Hz, C_8-H), 7.10—7.35 (4H, m, aromatic CH), 7.81 (1H, dd, J=2.2, 2.2 Hz, C_6-H)
IIIaf	1.35 (3H, br s, C_{8a}-Me), 1.79 and 1.88 (3H, br s, C_7-Me),[a] 4.15 (1H, br s, C_{4a}-H), 4.37 (1H, br s, C_{4b}-H), 4.97 (1H, br s, C_{1a}-H), 5.93 (1H, br s, C_8-H), 7.13—7.42 (4H, m, aromatic CH), 7.83 (1H, br s, C_6-H)
IIIag	1.34 (3H, s, C_{8a}-Me), 1.87 (3H, d, J=1.8 Hz, C_7-Me), 4.16 (1H, br s, C_{4a}-H), 4.35 (1H, br s, C_{4b}-H), 4.97 (1H, br s, C_{1a}-H), 5.92 (1H, d, J=1.8 Hz, C_8-H), 7.09—7.27 (3H, m, aromatic CH), 7.82 (1H, br s, C_6-H)
IIIah	1.36 (3H, s, C_{8a}-Me), 1.89 (3H, d, J=1.8 Hz, C_7-Me), 4.13 (1H, dd, J=9.0, 8.0 Hz, C_{4a}-H), 4.34 (1H, dd, J=9.0, 2.6 Hz, C_{4b}-H), 4.93 (1H, d, J=8.0 Hz, C_{1a}-H), 5.94 (1H, dd, J=1.8, 1.5 Hz, C_8-H), 7.14—7.36 (3H, m, aromatic CH), 7.83 (1H, dd, J=1.5, 2.6 Hz, C_6-H)
IIIai	1.36 (3H, s, C_{8a}-Me), 1.92 (3H, d, J=1.8 Hz, C_7-Me), 4.18 (1H, dd, J=9.0, 8.0 Hz, C_{4a}-H), 4.31 (1H, dd, J=9.0, 2.6 Hz, C_{4b}-H), 4.99 (1H, d, J=8.0 Hz, C_{1a}-H), 5.98 (1H, dd, J=1.8, 1.5 Hz, C_8-H), 7.06—7.26 (3H, m, aromatic CH), 7.86 (1H, dd, J=1.5, 2.6 Hz, C_6-H)

a) Split due to restricted rotation about o-FC_6H_4 group.

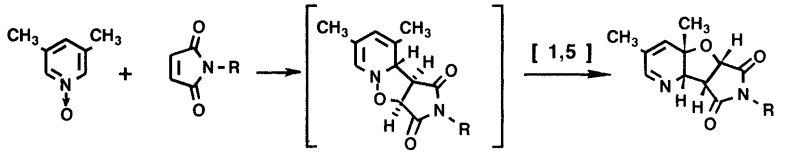

R

IIa: Ph
IIb: p-ClC_6H_4
IIc: p-MeC_6H_4
IId: p-FC_6H_4
IIe: m-FC_6H_4
IIf: o-FC_6H_4
IIg: p-Cl,o-FC_6H_3
IIh: m-Cl,p-FC_6H_3
IIi: o-Cl,p-FC_6H_3
IIj: n-butyl

Chart 1

of the *N*-butyl derivative (IIIaj).[4]

The crystal structure was solved by the direct method using the MULTAN78 series of programs.[5] Refinement to an *R* factor of 6.11% was obtained by the least-squares method on 2099 nonzero structure factors. As can be seen in the computer-generated drawing, IIIaj was confirmed to be an *endo* cycloadduct, providing definitive evidence of *exo* primary cycloaddition.

The torsion angles of H7–C7–C11–H11 and H11–C11–C12–H12 are 9.0° and 29.0°, respectively. These values are consistent with those calculated based on the coupling constants using the Karplus equation.[6] The torsion angle of N1–C2–C3–C4 is 12.4°, indicating that the 1-azadiene moiety is not planar. The C5–O6 bond length, 1.460 Å is greater than the O6–C7 bond length (1.423 Å). This elongation might be caused by steric repulsion between the *N*-substituted succinimide ring and the dihydropyridine moiety.

Cycloaddition of 2-Alkylpyridine *N*-Oxide with *N*-Substituted Maleimides Next, as an extension of the cycloaddition mentioned above, we carried out the reaction using 2-alkylpyridine *N*-oxides as 1,3-dipoles. In the reaction of 2,3-dimethylpyridine *N*-oxide (Ib), 2,5-dimethylpyridine *N*-oxide (Ic) and 5-ethyl-2-methylpyridine *N*-oxide (Id) with *N*-substituted maleimides (II), the reaction behaviors were different from the case of 3,5-dimethylpyridine *N*-oxide (Ia). The products obtained were revealed to be a series of cycloadducts of a new type (IV).

The high-resolution MS of IVba showed the molecular peak (M^+) at *m/z* 642.2087, which is consistent with the 1 : 3 adduct of Ib and IIa (calcd for $C_{37}H_{30}N_4O_7$: 642.2114).

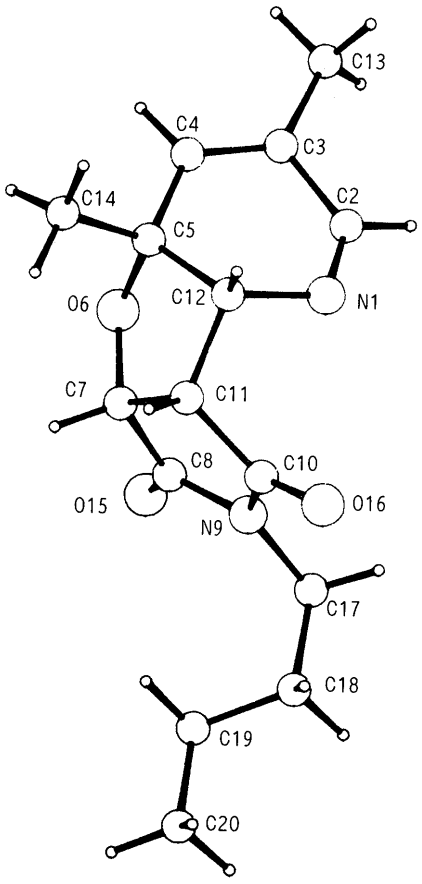

Fig. 1. Ortep Drawing of IIIaj

The IR spectrum of IVba showed a characteristic imido-carbonyl group absorption at 1720 cm^{-1}. The ^{13}C-nuclear magnetic resonance (^{13}C-NMR) spectrum of IVba exhibited ten sp^3 carbon signals from 18.3 to 75.7 ppm.[7] The ^1H-NMR spectrum of VIba exhibited one methyl signal at δ 1.60, one olefinic proton signal at δ 6.32 and four *cis*-oriented angular methine protons at δ 4.05—4.94. The details of the spectrum are depicted in Fig. 2. Inspection of the *J*-value between C_{4a}-H and C_{4b}-H indicates that IVba should be assigned as the *endo* product. The assignment was supported by the spectral behavior of the products (III) derived from the reaction of 3,5-

TABLE III. Fractional Atomic Coordinates[a] and Isotropic Temperature Factors (*B*) of IIIaj with Their Estimated Standard Deviations in Parentheses

Atom	*x/a*	*y/b*	*z/c*	*B*[b]
N1	−1647 (1)	6816 (2)	−2529 (3)	3.47 (5)
C2	−1165 (1)	7573 (3)	−2131 (4)	3.93 (7)
C3	−517 (1)	7096 (3)	−2103 (4)	3.91 (7)
C4	−410 (1)	5703 (4)	−2195 (4)	3.86 (7)
C5	−927 (1)	4637 (3)	−2393 (4)	3.35 (6)
O6	−1024 (1)	4164 (2)	−551 (3)	3.70 (4)
C7	−1646 (1)	3662 (3)	−614 (4)	3.17 (6)
C8	−1939 (1)	4270 (3)	991 (4)	3.45 (6)
N9	−2462 (1)	5029 (2)	319 (3)	3.49 (5)
C10	−2556 (1)	5061 (3)	−1572 (4)	3.32 (6)
C11	−2019 (1)	4304 (3)	−2299 (3)	3.02 (5)
C12	−1552 (1)	5316 (3)	−3095 (3)	3.17 (6)
C13	−19 (2)	8232 (4)	−1925 (6)	5.83 (10)
C14	−780 (1)	3337 (4)	−3532 (5)	4.97 (9)
O15	−1759 (1)	4133 (3)	2585 (3)	5.06 (6)
O16	−2999 (1)	5606 (2)	−2438 (3)	4.54 (5)
C17	−2878 (2)	5737 (4)	1490 (5)	4.77 (8)
C18	−3486 (2)	4936 (4)	1551 (5)	5.16 (9)
C19	−3422 (2)	3432 (4)	2309 (5)	5.15 (9)
C20	−4039 (2)	2675 (5)	2346 (5)	5.81 (10)
H2	−1233 (13)	8556 (31)	−1805 (38)	4.41 (65)
H4	4 (12)	5321 (30)	−2064 (36)	3.84 (60)
H7	−1669 (11)	2605 (28)	−574 (34)	3.09 (53)
H11	−2155 (12)	3548 (28)	−3102 (34)	3.25 (55)
H12	−1634 (11)	5317 (28)	−4367 (33)	3.00 (53)
H131	399 (16)	7815 (39)	−1890 (46)	6.72 (86)
H132	−73 (16)	8795 (40)	−972 (47)	6.85 (89)
H133	−28 (16)	8892 (39)	−2919 (47)	6.60 (86)
H141	−1126 (15)	2597 (36)	−3596 (43)	5.72 (76)
H142	−434 (14)	2852 (34)	−2938 (40)	4.92 (69)
H143	−721 (14)	3644 (34)	−4778 (41)	5.17 (72)
H171	−2651 (14)	5813 (33)	2614 (42)	5.14 (72)
H172	−2968 (14)	6698 (35)	938 (42)	5.42 (74)
H181	−3739 (15)	5542 (36)	2379 (44)	5.72 (77)
H182	−3700 (14)	4847 (34)	249 (40)	4.95 (70)
H191	−3156 (15)	2872 (36)	1521 (42)	5.52 (75)
H192	−3182 (16)	3585 (39)	3618 (48)	6.83 (88)
H201	−3990 (16)	1681 (39)	2907 (47)	6.85 (88)
H202	−4240 (15)	2653 (37)	1207 (44)	6.14 (81)
H203	−4312 (15)	3280 (36)	3019 (43)	5.78 (77)

a) Positional parameters are multiplied by 10^4. *b*) Thermal parameters are given as the equivalent temperature factors ($Å^2$).

TABLE IV. Bond Distances (Å) of IIIaj for Non-hydrogen Atoms with Their Estimated Standard Deviations in Parentheses

	Distance (Å)		Distance (Å)
N1–C2	1.265 (4)	N1–C12	1.468 (4)
C2–C3	1.471 (4)	C3–C4	1.311 (5)
C3–C13	1.502 (5)	C4–C5	1.489 (4)
C5–O6	1.460 (3)	C5–C12	1.531 (4)
C5–C14	1.518 (5)	O6–C7	1.423 (3)
C7–C8	1.509 (4)	C7–C11	1.525 (4)
C8–N9	1.379 (4)	C8–O15	1.201 (4)
N9–C10	1.384 (4)	N9–C17	1.467 (4)
C10–C11	1.506 (4)	C10–O16	1.203 (4)
C11–C12	1.541 (4)	C17–C18	1.518 (5)
C18–C19	1.498 (5)	C19–C20	1.513 (6)

TABLE V. Bond Angles (°) of IIIaj for Non-hydrogen Atoms with Their Estimated Standard Deviations in Parenthesis

	Angle (°)		Angle (°)
C2–N1–C12	116.7 (2)	N1–C1–C3	127.0 (3)
C2–C3–C4	118.0 (3)	C2–C3–C13	118.0 (3)
C4–C3–C13	124.0 (3)	C3–C4–C5	121.2 (3)
C4–C5–O6	106.9 (2)	C4–C5–C12	113.1 (2)
C4–C5–C14	112.1 (3)	O6–C5–C12	103.0 (2)
O6–C5–C14	109.6 (2)	C12–C5–C14	111.7 (2)
C5–O6–C7	107.4 (2)	O6–C7–C8	109.4 (2)
O6–C7–C11	108.5 (2)	C8–C7–C11	105.0 (2)
C7–C8–N9	108.0 (2)	C7–C8–O15	127.2 (3)
N9–C8–O15	124.8 (3)	C8–N9–C10	113.4 (2)
C8–N9–C17	123.4 (2)	C10–N9–C17	123.2 (3)
N9–C10–C11	108.2 (2)	N9–C10–O16	124.3 (3)
C11–C10–O16	127.6 (3)	C7–C11–C10	104.8 (2)
C7–C11–C12	103.4 (2)	C10–C11–C12	114.8 (2)
N1–C12–C5	116.0 (2)	N1–C12–C11	110.2 (2)
C5–C12–C11	102.6 (2)	N9–C17–C18	113.1 (3)
C17–C18–C19	114.7 (3)	C18–C19–C20	113.0 (3)

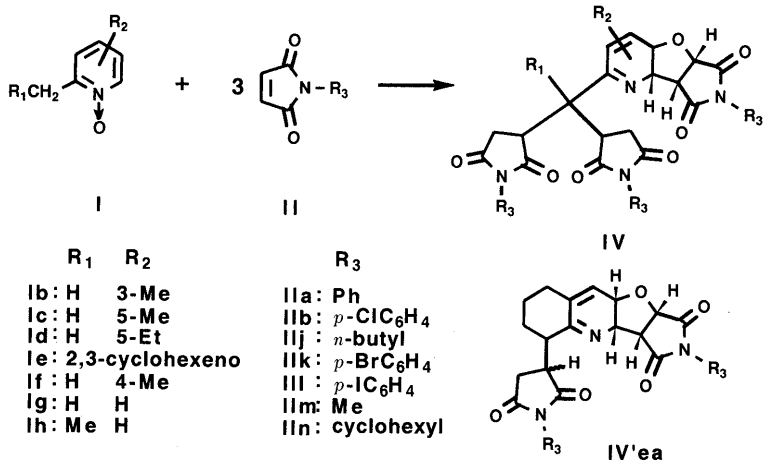

Chart 2

TABLE VI. Ene Reaction Products (IV) from the 1,3-Dipolar Reaction of 2-Alkylpyridine *N*-Oxide (Ia) with *N*-Substituted Maleimides (IIa—g)[a]

Product[b]	R	Yield (%)	mp (°C)	Formula	High-resolution MS Calcd (Found)	IR (cm^{-1}) C=O
IVba	Ph	18.3	254—255	$C_{37}H_{30}N_4O_7$	642.2114 (642.2087)	1720
IVbb	*p*-ClC_6H_4	24.1	250—251	$C_{37}H_{27}Cl_3N_4O_7$[c]		1712
IVbj	*n*-Butyl	20.0	175—177	$C_{31}H_{42}N_4O_7$	582.3053 (582.3029)	1698
IVbk	*p*-BrC_6H_4	22.2	259—261	$C_{37}H_{27}Br_3N_4O_7$[c]		1712
IVbl	*p*-IC_6H_4	17.1	239—241	$C_{37}H_{27}I_3N_4O_7$[c]		1712
IVbm	Me	25.7	248—249	$C_{22}H_{24}N_4O_7$	456.1645 (456.1633)	1692
IVbn	Cyclohexyl	20.5	254—255	$C_{37}H_{48}N_4O_7$	660.3523 (660.3522)	1704
IVca	Ph	32.7	226—227	$C_{37}H_{40}N_4O_7$	642.2114 (642.2144)	1704
IVcb	*p*-ClC_6H_4	24.1	234—236	$C_{37}H_{27}Cl_3N_4O_7$[c]		1710
IVcj	*n*-Butyl	41.5	141—142	$C_{31}H_{42}N_4O_7$	582.3053 (582.3035)	1694
IVck	*p*-BrC_6H_4	17.1	191—193	$C_{37}H_{27}Br_3N_4O_7$	876.9508 (876.9500)	1712
IVcl	*p*-IC_6H_4	14.7	190—192	$C_{37}H_{27}I_3N_4O_7$	1020.9090 (1020.8940)	1712
IVda	Ph	25.2	235—237	$C_{38}H_{32}N_4O_7$	656.2271 (656.2253)	1708

a) Refluxed for 10 h in toluene. *b*) Colorless needles, recrystallized from *n*-hexane–Me_2CO. *c*) Analyzed for C, H and N; the results were within ±0.3% of theoretical values.

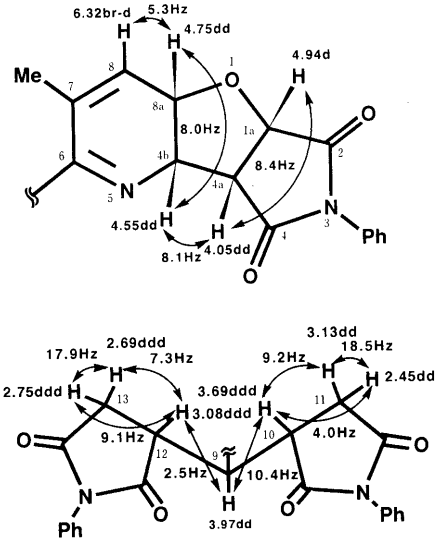

Fig. 2. ^{1}H-NMR Spectrum of IVba

dimethylpyridine *N*-oxide (Ia) with *N*-substituted maleimides (II), whose structures were confirmed by X-ray analysis.

As shown in Fig. 2, the two succinimide moieties exhibited ABX patterns. The spectral data for IVbb—da can be similarly assigned to the corresponding 1 : 3 ene reaction products (Tables VI and VII).

Attempts to isolate 1 : 1 cycloadducts by changing the I/II ratios were unsuccessful, giving rise only to the 1 : 3 ene reaction products (IV).

On the other hand, in the reaction of 2,3-cyclohexenopyridine *N*-oxide (Ie) with IIa, the 1 : 3 ene reaction product could not be obtained, but the 1 : 2 ene reaction product (IV'ea) was isolated as colorless needles (mp 179—182 °C) in 36.3% yield. The adduct (IV'ea) showed strong carbonyl absorption at 1714 cm^{-1} in the IR spectrum. The high-resolution MS spectrum of IV'ea showed M^+ at *m/z* 495.1794, which corresponds to the 1 : 2 ene reaction product of Ie and IIa. In the ^{1}H-NMR spectrum of IV'ea, digital integration showed the existence of twenty-five protons. The spectrum showed complex signals, presumably due to the existence of conformational isomers. As the temperature

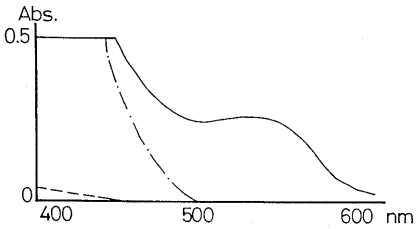

Fig. 3. Charge-Transfer Complex Formation in the Reaction of Ii with IIa

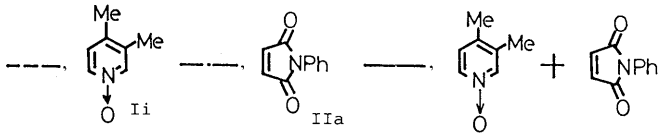

was raised, the signals became sharper but a completely averaged spectrum could not be obtained even at 100 °C. However, each of the proton signals was observed at a magnetic field consistent with the structure of IV'ea depicted in Chart 2. The ^{13}C-NMR spectrum of IV'ea also exhibited similar behavior (see Experimental). In the MS of IV'ea, the peak at *m/z* 477 ($M^+ - H_2O$) probably results from cleavage of an ether linkage followed by hydrogen rearrangement and elimination of water, leading to aromatization of the dihydropyridine ring. The fragmentation pattern is common in the adducts IV.

Charge Transfer Complex Formation In contrast, 2,4-dimethylpyridine *N*-oxide (If), 2-methylpyridine *N*-oxide (Ig), 2-ethylpyridine *N*-oxide (Ih) and 3,4-dimethylpyridine *N*-oxide (Ii) did not afford cycloadducts. In these cases, coloration due to charge-transfer (CT) complex formation was observed. When IIa was added to I in toluene solution, there was a marked intensification of the red color and the visible absorption spectrum of the mixture was different from the spectra of pure samples of the two solutes. This observation indicates that the reactions of I with II proceed *via* CT complex formation, which might play an important role in stabilizing the ground state.[8] In the cases of If—i, the reactions were stalled as a result of CT complex formation.[9]

Herbicidal Activity In the preliminary study, we found that the product (III) bearing the chloro substituent showed moderate herbicidal activity. So, we examined the herbicidal

TABLE VII. ^{1}H-NMR Spectral Data for the Ene Reaction Products (IV)[a]

Comp. No.	^{1}H-NMR δ (400 MHz)
IVba[b]	1.60 (3H, br s, C_7-Me), 2.45 (1H, dd, J=4.0, 18.5 Hz, C_{11}-H), 2.75 (1H, dd, J=7.3, 17.9 Hz, C_{13}-H), 2.69 (1H, dd, J=9.1, 17.9 Hz, C_{13}-H), 3.08 (1H, ddd, J=2.5, 7.3, 9.1 Hz, C_{12}-H), 3.13 (1H, dd, J=9.2, 18.5 Hz, C_{11}-H), 3.69 (1H, ddd, J=4.0, 9.2, 10.4 Hz, C_{10}-H), 3.97 (1H, dd, J=2.5, 10.4 Hz, C_9-H), 4.05 (1H, dd, J=8.1, 8.4 Hz, C_{4a}-H), 4.55 (1H, dd, J=8.1, 8.0 Hz, C_{4b}-H), 4.75 (1H, dd, J=8.0, 5.3 Hz, C_{8a}-H), 4.94 (1H, d, J=8.4 Hz, C_{1a}-H), 6.32 (1H, br d, J=5.3 Hz, C_8-H), 7.18—7.50 (15H, m, aromatic CH)
IVbb[c]	2.03 (3H, br s, C_7-Me), 2.26 (1H, dd, J=4.5, 17.9 Hz, C_{11}-H), 2.38 (1H, dd, J=8.4, 17.9 Hz, C_{11}-H), 2.73 (1H, dd, J=6.8, 17.6 Hz, C_{13}-H), 2.89 (1H, dd, J=9.5, 17.6 Hz, C_{13}-H), 3.17—3.23 (1H, m, C_{10}-H), 3.62 (1H, ddd, J=4.5, 8.4, 10.3 Hz, C_{12}-H), 3.99 (1H, br d, J=10.4 Hz, C_9-H), 4.19 (1H, dd, J=8.1, 8.4 Hz, C_{4a}-H), 4.39—4.43 (2H, m, C_{4b}-H, C_{8a}-H), 4.93 (1H, d, J=8.1 Hz, C_{1a}-H), 6.40 (1H, br d, J=4.4 Hz, C_8-H), 7.14—7.58 (12H, m, aromatic CH)
IVbj[c]	0.89—0.95 (9H, m, $-CH_2CH_2CH_2CH_3$), 1.23—1.39 (6H, m, three $-CH_2CH_2CH_2CH_3$), 1.44—1.63 (6H, m, three $-CH_2CH_2CH_2CH_3$), 2.00 (3H, br s, C_7-Me), 2.28 (1H, dd, J=18.3, 4.8 Hz, C_{11}-H), 2.44 (1H, dd, J=17.6, 9.2 Hz, C_{13}-H), 2.53 (1H, dd, J=17.6, 6.6 Hz, C_{13}-H), 2.81 (1H, dd, J=18.3, 9.5 Hz, C_{11}-H), 2.81 (1H, ddd, J=10.3, 9.2, 6.6 Hz, C_{12}-H), 3.29 (1H, ddd, J=9.5, 9.5, 4.8 Hz, C_{10}-H), 3.38—3.57 (6H, m, three $-CH_2CH_2CH_2CH_3$), 3.75 (1H, m, C_9-H), 3.90 (1H, dd, J=8.4, 8.4 Hz, C_{4a}-H), 4.30 (1H, dd, J=8.4, 8.4 Hz, C_{4b}-H), 4.35 (1H, dd, J=5.5, 8.4 Hz, C_{8a}-H), 4.75 (1H, d, J=8.4 Hz, C_{1a}-H), 6.26 (1H, dd, J=1.5, 5.5 Hz, C_8-H)
IVbk[c]	2.03 (3H, br s, C_7-Me), 2.27 (1H, dd, J=6.8, 17.5 Hz, C_{11}-H), 2.38 (1H, dd, J=9.3, 17.5 Hz, C_{11}-H), 2.73 (1H, dd, J=5.1, 18.0 Hz, C_{13}-H), 2.89 (1H, dd, J=8.9, 18.0 Hz, C_{13}-H), 3.18—3.21 (1H, m, C_{10}-H), 3.61 (1H, ddd, J=5.1, 8.9, 8.9 Hz, C_{12}-H), 3.99 (1H, br d, J=8.9 Hz, C_9-H), 4.19 (1H, dd, J=8.1, 8.4 Hz, C_{4a}-H), 4.38—4.43 (2H, m, C_{4b}-H, C_{8a}-H), 4.93 (1H, d, J=8.4 Hz, C_{1a}-H), 6.40 (1H, br d, J=5.1 Hz, C_8-H), 7.14—7.58 (12H, m, aromatic CH)
IVbl[b]	2.02 (3H, br s, C_7-Me), 2.26 (1H, dd, J=4.8, 17.4 Hz, C_{11}-H), 2.40 (1H, dd, J=8.6, 17.4 Hz, C_{11}-H), 2.72 (1H, dd, J=6.8, 17.9 Hz, C_{13}-H), 2.87 (1H, dd, J=9.3, 17.9 Hz, C_{13}-H), 3.16—3.22 (1H, m, C_{10}-H), 3.55—3.62 (1H, m, C_{12}-H), 3.97 (1H, br d, J=9.9 Hz, C_9-H), 4.17 (1H, dd, J=8.1, 8.4 Hz, C_{4a}-H), 4.37—4.43 (2H, m, C_{4b}-H, C_{8a}-H), 4.91 (1H, d, J=8.4 Hz, C_{1a}-H), 6.37 (1H, br d, J=3.7 Hz, C_8-H), 6.92—7.88 (12H, m, aromatic CH)
IVbm[b]	1.97 (3H, br s, C_7-Me), 2.17 (1H, dd, J=17.6, 9.2 Hz, C_{13}-H), 2.28 (1H, dd, J=17.6, 6.2 Hz, C_{13}-H), 2.56 (2H, d, J=6.8, 17.9 Hz, C_{11}-H), 2.72 (3H, s, *N*-Me), 2.80 (3H, s, *N*-Me), 2.82 (3H, s, *N*-Me), 2.93 (1H, ddd, J=6.2, 9.2, 9.9 Hz, C_{12}-H), 3.20 (1H, d, J=16.5, 6.8 Hz, C_{10}-H), 3.74 (1H, br d, J=9.9 Hz, C_9-H), 3.99 (1H, dd, J=8.1, 8.4 Hz, C_{4a}-H), 4.18—4.25 (2H, m, C_{4b}-H, C_{8a}-H), 4.69 (1H, d, J=8.4 Hz, C_{1a}-H), 6.30 (1H, br d, J=5.5 Hz, C_8-H)
IVbn[c]	1.12—2.17 (30H, m, methylene protons of cyclohexyl), 1.95 (3H, s, C_7-Me), 2.45 (1H, dd, J=18.0, 4.4 Hz, C_{13}-H), 2.63—2.77 (3H, m, C_{13}-H, C_{11}-H), 2.92 (1H, ddd, J=7.0, 3.7, 9.2 Hz, C_{10}-H), 3.27 (1H, ddd, J=4.4, 4.4, 8.8 Hz, C_{12}-H), 3.66—3.71 (1H, m, C_9-H), 3.68 (1H, dd, J=8.1, 9.2 Hz, C_{4a}-H), 3.84—4.00 (3H, m, methine protons of cyclohexyl), 4.41 (1H, m, C_{4b}-H), 4.46 (1H, m, C_{8a}-H), 4.64 (1H, d, J=8.1 Hz, C_{1a}-H), 6.06 (1H, dd, J=4.4, 1.7 Hz, C_8-H)
IVca[c]	1.33 (3H, s, C_{8a}-Me), 2.62 (1H, dd, J=4.8, 18.8 Hz, C_{11}-H), 2.96 (1H, dd, J=11.7, 20.2 Hz, C_{13}-H), 3.12 (1H, dd, J=9.4, 18.8 Hz, C_{11}-H), 3.18 (1H, m, C_{12}-H), 3.21 (1H, m, C_{13}-H), 3.58 (1H, ddd, J=2.5, 4.8, 9.4 Hz, C_{10}-H), 3.74 (1H, dd, J=2.5, 6.2 Hz, C_9-H), 3.86 (1H, dd, J=7.7, 9.9 Hz, C_{4a}-H), 4.52 (1H, d, J=9.9 Hz, C_{4b}-H), 4.89 (1H, d, J=7.7 Hz, C_{1a}-H), 5.87 (1H, d, J=9.9 Hz, C_7-H), 6.35 (1H, d, J=9.9 Hz, C_8-H), 7.12—7.46 (15H, m, aromatic CH)
IVcb[b]	1.23 (3H, s, C_{8a}-Me), 2.73—2.95 (4H, m, C_{11}-H, C_{13}-H), 3.51 (1H, br s, C_{10}-H), 3.59—3.63 (2H, m, C_9-H, C_{12}-H), 4.05 (1H, dd, J=7.9, 9.7 Hz, C_{4a}-H), 4.50 (1H, d, J=9.7 Hz, C_{4b}-H), 4.91 (1H, d, J=7.9 Hz, C_{1a}-H), 6.08 (1H, d, J=9.7 Hz, C_7-H), 6.39 (1H, d, J=9.7 Hz, C_8-H), 7.24—7.58 (12H, m, aromatic CH)
IVcj[c]	0.89—0.95 (9H, m, three $-CH_2CH_2CH_2CH_3$), 1.24 (3H, s, C_{8a}-Me), 1.25—1.62 (12H, m, three $-CH_2CH_2CH_2CH_3$), 2.47 (1H, dd, J=18.0, 5.1 Hz, C_{13}-H), 2.85—2.95 (1H, m, C_{11}-H), 2.88 (1H, dd, J=18.0, 8.5 Hz, C_{13}-H), 3.01—3.07 (1H, m, C_{11}-H), 3.09 (1H, dd, J=3.3, 5.9 Hz, C_{10}-H), 3.26—3.36 (1H, m, C_{12}-H), 3.32—3.51 (6H, m, three $-CH_2CH_2CH_2CH_3$), 3.58 (1H, dd, J=5.9, 2.9 Hz, C_9-H), 3.68 (1H, dd, J=7.7, 9.9 Hz, C_{4a}-H), 4.31 (1H, d, J=9.9 Hz, C_{4b}-H), 4.74 (1H, d, J=7.7 Hz, C_{1a}-H), 5.66 (1H, J=9.9 Hz, C_7-H), 6.12 (1H, J=9.9 Hz, C_8-H)
IVck[b]	1.22 (3H, s, C_{8a}-Me), 2.72—2.93 (4H, m, C_{11}-H, C_{13}-H), 3.48—3.53 (1H, m, C_{10}-H), 3.58—3.65 (2H, m, C_9-H, C_{12}-H), 4.04 (1H, dd, J=7.7, 9.9 Hz, C_{4a}-H), 4.49 (1H, d, J=9.9 Hz, C_{4b}-H), 4.89 (1H, d, J=7.7 Hz, C_{1a}-H), 6.06 (1H, d, J=9.9 Hz, C_7-H), 6.39 (1H, d, J=9.9 Hz, C_8-H), 7.16—7.71 (12H, m, aromatic CH)
IVcl[b]	1.22 (3H, s, C_{8a}-Me), 2.75—2.88 (4H, m, C_{11}-H, C_{13}-H), 3.44—3.52 (1H, m, C_{10}-H), 3.55—3.63 (2H, m, C_9-H, C_{12}-H), 4.03 (1H, dd, J=7.7, 9.9 Hz, C_{4a}-H), 4.48 (1H, d, J=9.9 Hz, C_{4b}-H), 4.88 (1H, d, J=7.7 Hz, C_{1a}-H), 6.04 (1H, d, J=9.9 Hz, C_7-H), 6.36 (1H, d, J=9.9 Hz, C_8-H), 7.16—7.71 (12H, m, aromatic CH)
IVda[b]	0.78 (3H, t, J=7.5 Hz, C_{8a}-CH_2CH_3), 1.50—1.62 (2H, m, C_{8a}-CH_2CH_3), 2.71 (1H, dd, J=9.2, 17.8 Hz, C_{13}-H), 2.80—2.86 (3H, m, C_{13}-H, C_{11}-H), 3.54—3.60 (2H, m, C_{10}-H, C_{12}-H), 3.67—3.70 (1H, m, C_9-H), 4.08 (1H, dd, J=7.5, 10.4 Hz, C_{4a}-H), 4.58 (1H, d, J=10.4 Hz, C_{4b}-H), 4.91 (1H, d, J=7.5 Hz, C_{1a}-H), 6.20 (1H, d, J=10.1 Hz, C_7-H), 6.39 (1H, d, J=10.1 Hz, C_8-H), 7.18—7.50 (15H, m, aromatic CH)

a) Numbering sequence: see Fig. 2. *b*) In DMSO-d_6. *c*) In $CDCl_3$.

activities of other cycloadducts in the series.

The *N*-(*p*-chlorophenyl) derivative (IIIab) showed herbicidal activity against Green Amaranth, with 100% blighting at 4 ppm. Furthermore, the *N*-(*p*-tolyl) derivative (IIIac) was effective against monocotyledons (43% blighting) and against Foxtail green (85% blighting) at 4 ppm.

The biological activities of IV could not be examined in aqueous solution, because the compounds are not soluble in water. The biological activities of IV in non-aqueous solutions are under investigation, and the results will be published in the near future.

Discussion

As hitherto mentioned, in the case of 3,5-dimethylpyridine *N*-oxide (Ia), the pericyclic reaction afforded 2,3-dihydrofuro[3,2-*b*]pyridines (III) as final products. On the other hand, 2-alkylpyridine *N*-oxides (Ib—e) gave 1 : 3 (or 1 : 2) ene reaction products (IV). The difference in the pericyclic reaction behavior can be ascribed to the existence of the α-methyl group on the pyridine nucleus.

Next, mention should be made of the formation mechanism of the 1 : 3 ene reaction product, taking into consideration previously reported mechanistic aspects of analogous reactions.[10] The formation mechanism of the 1 : 3 ene reaction products can be analyzed by dividing the whole reaction into four steps from the frontier molecular orbital (FMO) theoretical point of view[11] (Chart 3). The first step of the reaction is the concerted 1,3-cycloaddition

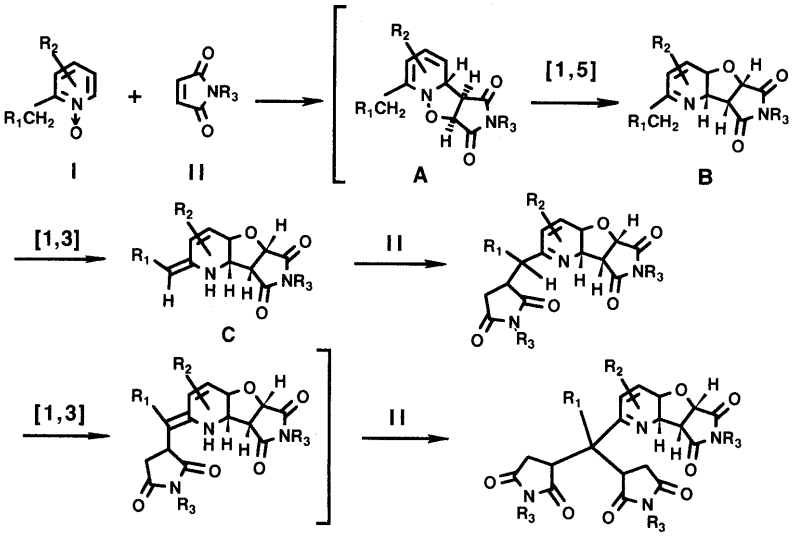

Chart 3

of I with II. Molecular orbital calculations based on the modified neglect of diatomic overlap (MNDO) approximation[12] were performed and the results are summarized in Fig. 4. Sustmann[13] has classified 1,3-dipolar cycloadditions into three general types according to the highest occupied molecular orbital (HOMO)–lowest unoccupied molecular orbital (LUMO) arrangement of the 1,3-dipole and dipolarophile. They are the normal electron demand, the inverse electron demand, and the neutral electron demand types. The normal electron demand reaction is dominated by the interaction of the HOMO of the 1,3-dipole and the LUMO of the dipolarophile. As can be seen in Fig. 4, the first step of the reaction of I with II falls into the category of a normal electron demand reaction in Sustmann's classification, wherein the dominant interaction occurs between the HOMO of I and the LUMO of II.

In the 2,3-dihydrofuro[3,2-*b*]pyridine skeleton of the 1 : 3 ene reaction product, four *cis* oriented angular methine protons were observed. This suggests that the primary cycloaddition of I with II proceeds *via* the *exo* transition state, in which unfavorable secondary orbital interactions[2b,4] do not occur.

The second step of the reaction can be explained by the sigmatropic 1,5-shift of the primary cycloadduct (A) to the rearrangement product (B). Based on the structure optimization data for simple model compounds (type A and type B), the latter is considered to be more stable by about 30 kcal/mol than the former in terms of the heat of formation.[14]

The third step of the reaction is 1,3-sigmatropic hydrogen shift of the rearrangement product (B) to the enamine-type compound (C). Though the suprafacial 1,3-sigmatropy is a forbidden process under thermal conditions, the lone pair

The fourth step of the reaction is the attack of the second molecule of the maleimide on the enamine-type compound (C), commonly referred to as the "ene reaction". From the MNDO calculations on the heterodiene-type model compound (D) and enamine-type model compound (E) shown in Fig. 5, the HOMO orbital of E lies 1.28 eV higher than that of D, indicating that ene reaction of E with II is more advantageous than hetero-Diels–Alder reaction of D with II.[11b] It can be suggested that the marked increase of

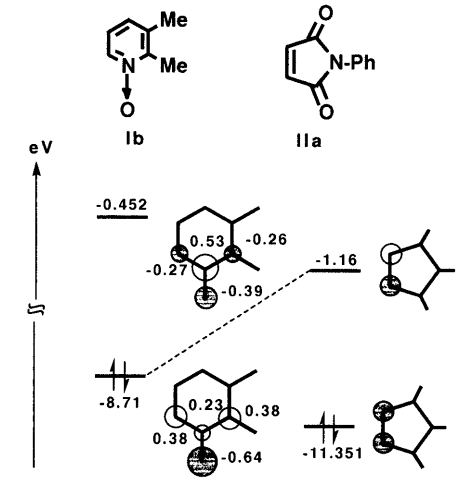

Fig. 4. MNDO Calculation of 2,3-Dimethylpyridine *N*-Oxide (Ib) and *N*-Phenylmaleimide (IIa)

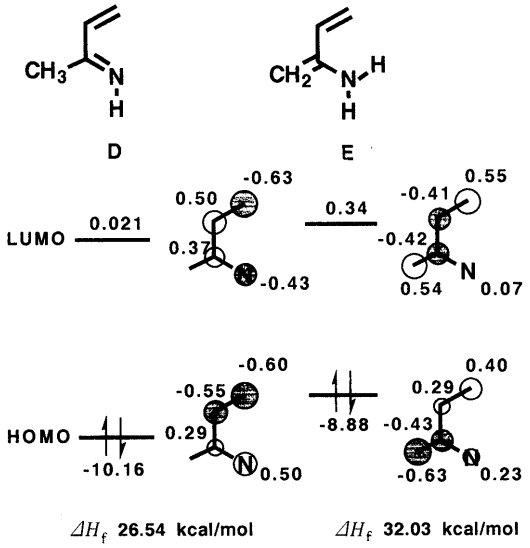

Fig. 5. MNDO Calculation of Model Compounds (D and E)

on the ring nitrogen is in phase with the lobe of the hydrogen on the α-Me group, which makes it possible for the proton to migrate to the ring nitrogen.

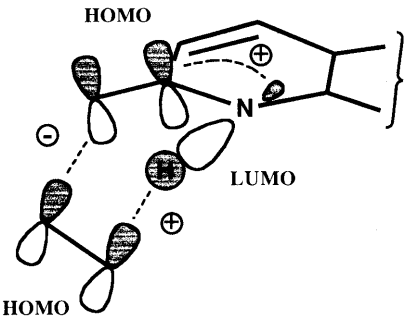

Fig. 6. Three System Interaction in the Third Step of the Reaction

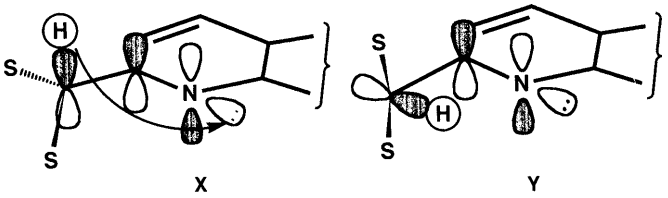

S: 3-(*N*-substituted)-succinimido

Fig. 7. Plausible Conformations for 1,3-Hydrogen Shift

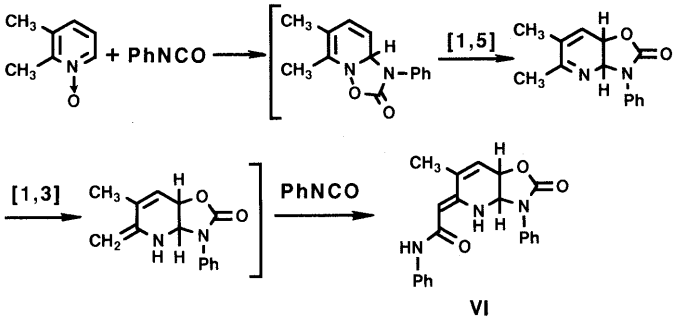

Chart 4

the HOMO level increases the perturbation energy and compensates for the 5.49 kcal/mol $\{\Delta H_f(E) - \Delta H_f(D)\}$ disadvantage in heat of formation.[11a] The magnitude of the HOMO coefficients of the enamine-type model compound (E) is greatest upon the exocyclic terminal methylene carbon, and therefore the second molecule of the maleimide attacks the methylene carbon.

The mode of this step can be rationalized in terms of a three system interaction[15] as depicted in Fig. 6. In this case, the exocyclic methylene moiety (π-HOMO) and double bond (π-HOMO) of maleimides participate in the reaction as donors, and the N–H σ-bond works as an acceptor (σ-LUMO). In the same manner, 1,3-sigmatropic hydrogen shift might be repeated when the third molecule of maleimide attacks the exocyclic methylene moiety.

In this step, the migrating hydrogen atom has to take a conformation (X) in which the C–H σ-bond lies in parallel with the lobe of the *Pz* orbital. In the case of the disubstituted compounds (Y), the steric interference between the *N*-substituted succinimide rings and the 2,3-dihydropyridine moiety prevents the parallel arrangement. Therefore, a fourth molecule of II could not participate in the reaction. Similarly, for the reaction of Ig, only the 1 : 2 adduct (IV'ea) could be obtained.

In connection with this reaction, the reaction of 2,3-dimethylpyridine with IIa was examined and afforded 2-[3-(*N*-phenylsuccinimido)methyl]-3-methylpyridine (V) in 34% yield.

As mentioned in the previous papers,[9] the cycloaddition of 2-alkylpyridine *N*-oxides (Ib, c) with phenyl isocyanates resulted in the formation of 1 : 2 cycloadducts (VI) and the pathway for the formation of the 1 : 2 cycloadducts may be explained in the same manner as mentioned above.

Experimental

All melting points are uncorrected. ^{1}H-NMR spectra were taken with Hitachi R-600 (60 MHz) and JEOL GX-400 (400 MHz) spectrometers for *ca.* 10% (w/v) solution with tetramethylsilane (TMS) as an internal standard; chemical shifts are expressed in δ values. IR spectra were recorded on a Hitachi 270-30 infrared spectrophotometer equipped with a double-blade grating. Visible absorption spectra were taken with a Hitachi 150-20 spectrometer. MS were taken with a JEOL JMS-DX303HF double-focussing spectrometer operating at an ionization potential of 75 eV. Molecular orbital calculations were performed on a FACOM M-360 computer at the Information Processing Center of Kumamoto University. Graphic analysis of the MO calculation and X-ray data were performed on a FACOM G-150 work station and a Fujitsu FM R-60HD personal computer.

Materials 3,5-Dimethylpyridine *N*-oxide (Ia), 2,3-dimethylpyridine *N*-oxide (Ib), 2,5-dimethylpyridine *N*-oxide (Ic), 5-ethyl-2-methylpyridine *N*-oxide (Id), 2,3-cyclohexenopyridine *N*-oxide (Ie), 2,4-dimethylpyridine *N*-oxide (If), 2-methylpyridine *N*-oxide (Ig), 2-ethylpyridine *N*-oxide (Ih) and 3,4-dimethylpyridine *N*-oxide (Ii) were prepared according to the established methods.[16] *N*-Substituted maleimides (IIa—n) were also prepared according to the established methods.[17]

Reaction of 3,5-Dimethylpyridine *N*-Oxides (Ia) with *N*-Substituted Maleimides (II). General Procedures A solution of Ia (0.01 mol) and II (0.02 mol) in 10 ml of absolute toluene was refluxed for 10 h. After cooling, the solution was concentrated *in vacuo*. The residue was purified by column chromatography on silica gel using AcOEt as an eluent to give III, which was purified by recrystallization (see Tables I and II).

Reaction of 2-Alkyl Substituted Pyridine *N*-Oxides (Ib—i) with *N*-Substituted Maleimides (II). General Procedures A solution of I (0.01 mol) and II (0.03 mol) in 10 ml of absolute toluene was refluxed for 10 h. After cooling, the solution was concentrated *in vacuo*. The residue was purified by column chromatography on silica gel using AcOEt as an eluent to give IV, which was purified by recrystallization (see Tables VI and VII).

According to the general procedure, Ie was allowed to react with IIa to give IV'ea in 36.4% yield, mp 184—186 °C (Me_2CO, colorless powder). IR (KBr): 1714 (C=O) cm^{-1}. MS *m/z*: 495 (M^+), 477 ($M^+ - H_2O$). High-resolution MS *m/z*: 495.179 (M^+, Calcd for $C_{29}H_{25}N_3O_5$: 495.180). ^{1}H-NMR (in DMSO-d_6 at 100 °C) δ: 1.56—1.79 (2H, m, C_{10}-H), 2.02—2.24 (2H, m, C_{14}-H), 2.49—3.06 (4H, m, C_{11}-H, C_{12}-H), 3.47—3.50 (1H, m, C_{13}-H), 3.66—3.70 (1H, m, C_9-H), 4.01—4.03 (1H, m, C_{4a}-H), 4.43—4.47 (1H, m, C_{4b}-H), 4.58 (1H, br s, C_{8a}-H), 4.80 (1H, d, J=8.1 Hz, C_{1a}-H), 6.01 (1H, br s, C_8-H), 7.14—7.47 (10H, m, aromatic CH). ^{13}C-NMR (in DMSO-d_6 at 100 °C) δ: 29.69, 30.89 (br s), 31.36, 32.21 (br s), 44.84, 45.72, 48.40, 49.36, 73.3, 75.7, 132.33, 132.76 (br s), 132.97, 167.18, 172.59 (br s), 174.56 (br s), 176.56 (br s). Phenyl carbons were observed in the range of δ 126.17—128.99.

Reaction of 2,3-Dimethylpyridine with *N*-Phenylmaleimide (IIa) A solution of IIa (0.01 mol) in 5 ml of 2,3-dimethylpyridine was heated at 120 °C for 6 h. After cooling, the excess 2,3-dimethylpyridine was removed under reduced pressure. The residue was purified by column chromatography on silica gel using C_6H_6–AcOEt (1 : 1) as an eluent to give crude V, which was purified by recrystallization from AcOEt to give V as colorless prisms (34% yield), mp 124—126 °C. IR (KBr): 1708 cm^{-1}. ^{1}H-NMR ($CDCl_3$) δ: 2.30 (3H, s, C_3-Me), 2.78 (1H, dd, J=4.8, 17.4 Hz, methylene proton of succinimide), 3.03 (1H, dd, J=9.4, 17.4 Hz, methylene proton of succinimide), 3.28—3.34 (1H, m, methine proton of succinimide), 3.41—3.50 (2H, m, C_2-CH_2), 7.04—7.07 (1H, m, C_4-H), 7.25—7.50 (6H, m, C_5-H and phenyl CH), 8.27—8.29 (1H, m, C_6-H). High-resolution MS *m/z*: 280.1193 (M^+, Calcd $C_{17}H_{16}N_2O_2$: 280.1212).

X-Ray Crystallography Crystal data. $C_{15}H_{20}N_2O_3$ (IIIaj): monoclinic $P2_1/n$, a=21.691 (11) Å, b=9.240 (4) Å, c=7.356 (4) Å, β=96.27 (4)°, V=1465.5 (12) Å^3, D_m=1.238 g cm^{-3} (aq. KI), D_c=1.253 g cm^{-3}, Z=4, Mo K_α radiation (40 kV, 20 mA), λ=0.7107 Å.

The cell constants were determined by a least-squares procedure using the value of the Bragg angles of 17 reflections measured on a Rigaku AFC-6 four-circle autodiffractometer equipped with a graphite-monochromated Mo K_α source, and interfaced to a PANAFACOM U-1200 minicomputer.

The space group $P2_1/n$ was selected from the number of molecules per unit cell ($Z=4$) and was later confirmed in the course of the structure refinement. Intensity data were collected in the range $2\theta<60°$ using the θ–2θ scan technique. A variable scan rate was adopted. Two reflections were monitored after measurement of every 100 reflections. Of the 3174 independent reflections, 2467 were treated as observed ($F_O>3\sigma F$). The intensities were corrected for Lorentz and polarization effects, but no correction was applied for absorption.

Structure Solution and Refinement An overall temperature factor obtained from a Wilson plot did not give the correct solution. Therefore, the value of 5.0 Å^2 was used to calculate normalized structure factor. The structure was solved by the direct method using the MULTAN78 series of programs. An E map calculated with 390 signed E's ($E>1.2$), which gave a combined figure of merit of 2.255, revealed the positions of all the expected nonhydrogen atoms. Refinements were carried out by the block-diagonal least-squares method. Six cycles of isotropic refinement and 6 cycles of anisotropic refinement led to an R index of 0.106. All the hydrogens were located at calculated positions. After adding the hydrogens and isotropic refinement for hydrogens, we obtained a final R of 0.061. Thermal parameters of the hydrogens were refined with calculated shifts damped by a factor of 0.1. In final refinements, 2099 reflections with $2\theta<55°$ were used and the following weights were applied to the observed reflections: $w=1.0$ for $F_O<20.0$, $w=400/F_O^2$ for $F_O>20.0$.

All structure-solving programs were from the Information Processing Center of Kumamoto University (Universal Crystallographic Computation Program System, UNICS III).[18]

Measurement of Visible Absorption Spectra Solutions of Ii (1 mmol/l) and IIa (1 mmol/l) in dry C_6H_6 were used for the measurement at 25 °C. The results are shown in Fig. 3.

Acknowledgement The authors wish to express their thanks to the members of the Analytical Department of the Faculty of Pharmaceutical Sciences, Kumamoto University. They are also grateful to Mr. Nakatomi, President of Hisamitsu Pharmaceutical Co., Inc., for partial financial support.

References and Notes

1) *a*) T. Matsuoka, M. Shinada, F. Suematsu, K. Harano and T. Hisano, *Chem. Pharm. Bull.*, **32**, 2077 (1984) and references cited therein; *b*) K. Harano, R. Kondo, M. Murase, T. Matsuoka and T. Hisano, *ibid.*, **34**, 966 (1986); *c*) K. Harano, F. Suematsu, T. Matsuoka and T. Hisano, *ibid.*, **32**, 543 (1984).
2) *a*) T. Matsuoka, K. Harano and T. Hisano, *Chem. Pharm. Bull.*, **31**, 2948 (1983); *b*) T. Hisano, K. Harano, T. Matsuoka, H. Yamada and M. Kurihara, *ibid.*, **35**, 1049 (1987).
3) *a*) T. Hisano, K. Harano, T. Matsuoka, S. Watanabe and T. Matsuzaki, *Chem. Pharm. Bull.*, **37**, 907 (1989); *b*) Y. Tamura, Y. Miki and M. Ikeda, *J. Chem. Soc., Perkin Trans. 1*, **1976**, 1702.
4) K. Harano, T. Matsuoka, M. Eto, T. Matsuzaki and T. Hisano, *Heterocycles*, **29**, 1029 (1989).
5) P. Main, S. E. Hull, L. Lessinger, G. Germain, J. P. Declercq and M. M. Moolfson, "MULTAN78, A System of Computer Programs for the Automatic Solution of Crystal Structure from X-Ray Diffraction Data," Univ. of York, England, 1978.
6) M. Karplus, *J. Chem. Phys.*, **30**, 11 (1959).
7) Chemical shifts of sp^3 carbons (in dimethyl sulfoxide-d_6 (DMSO-d_6), ppm): 18.3, 30.3, 34.4, 38.2, 41.2, 42.1, 50.9, 61.2, 73.1, 75.7.
8) K. Mok and M. J. Nye, *J. Chem. Soc., Perkin Trans. 1*, **1975**, 1810.
9) Concerning with the CT-complex formation, Mok and Nye[8] suggested that whether the cycloaddition does occur or not depends upon the relative stabilities of the ground state and transition state. We obtained some results which support their suggestion experimentally, *i.e.* the cycloaddition of pyridine *N*-oxides with phenyl isocyanates or *N*-phenylmaleimides proceeds, whereas that with 4-phenyl-1,2,4-triazoline-3,5-dione or tetracyanoethylene does not. In the latter cases, charge transfer might be sufficiently great that the reaction course might be altered to result in a stepwise reaction (substitution reaction) or formation of a stable CT-complex which could not transform into the corresponding cycloadduct.[1b]
10) *a*) T. Hisano, M. Ichikawa, T. Matsuoka, K. Muraoka and M. Hamana, *Org. Prep. Proced. Int.*, **13**, 409 (1981); *b*) T. Matsuoka, K. Harano, H. Kubo and T. Hisano, *Chem. Pharm. Bull.*, **34**, 572 (1986).
11) *a*) K. Fukui, "Kagaku Hanno To Densi No Kido (Chemical Reactions and Electron Orbitals)," Maruzen, Tokyo, 1976; *b*) I. Fleming, "Frontier Orbitals and Organic Chemical Reactions," John Wiley & Sons, Ltd., London, 1976, pp. 106—109.
12) M. J. S. Dewar and W. Thiel, *J. Am. Chem. Soc.*, **99**, 4899, 4907 (1977); M. J. S. Dewar and J. J. P. Stewart, "Quantum Chemistry Program Exchange (QCPE), Program No. 464," Indiana University, 1984.
13) R. Sustmann, *Tetrahedron Lett.*, **1971**, 2717, 2721.
14) Calculations on a model cycloadduct of pyridine *N*-oxide with ethylene indicate that the heat of formation (ΔH) of the 1,5-sigmatropy product is 26.7 kcal/mol smaller than that of the primary one, suggesting the primary adduct to be thermodynamically less stable.[2]
15) S. Inagaki, H. Fujimoto and K. Fukui, *J. Am. Chem. Soc.*, **98**, 4693 (1976).
16) E. Ochiai, "Aromatic Amine Oxides," Elsevier Publishing Co., Amsterdam, 1967.
17) M. P. Cava, A. A. Deana, K. Muth and M. J. Mitchell, *Org. Syn. Coll. Vol.*, **5**, 944 (1973).
18) T. Sakurai and K. Kobayashi, *Rikagaku Kenkyusho Hokoku*, **55**, 69 (1979); S. Kawano, *Koho, Comput. Center Kyushu Univ.*, **16**, 113 (1983).